Asteroids: New Observations, New Models
Proceedings IAU Symposium No. 318, 2015
S. R. Chesley, A. Morbidelli, R. Jedicke & D. Farnocchia, eds.

doi:10.1017/S1743921315008790

Direct Detections of the Yarkovsky Effect: Status and Outlook

Steven R. Chesley[1], Davide Farnocchia[2], Petr Pravec[3] and David Vokrouhlický[4]

[1]Jet Propulsion Laboratory
California Institute of Technology
Pasadena, CA 91109 USA
email: steve.chesley@jpl.nasa.gov

[2]Jet Propulsion Laboratory
California Institute of Technology
Pasadena, CA 91109 USA
email: davide.farnocchia@jpl.nasa.gov

[3]Astronomical Institute
The Czech Academy of Sciences
CZ-251 65 Ondřejov, Czech Republic
email: petr.pravec@asu.cas.cz

[4]Institute of Astronomy
Charles University
CZ-180 00 Prague 8, Czech Republic
email: vokrouhl@cesnet.cz

Abstract. We report the current results on a comprehensive scan of the near-Earth asteroid catalog for evidence of the Yarkovsky effect in the orbital motion of these bodies. While most objects do not have sufficient observational data to reveal such slight acceleration, we do identify 42 asteroids with a "valid" detection of the Yarkovsky effect, i.e., those with a signal at least 3 times greater than the formal uncertainty and a value compatible with the Yarkovsky mechanism.

We also identify a special category of non-detection, which we refer to as "weak signal," where the objects are of a size that would permit a clear detection if the Yarkovsky effect is maximized, and yet the orbit is clearly incompatible with such accelerations. The implication is that the Yarkovsky effect is reduced in these cases, presumably due to mid-range obliquity, but possibly also due to size, bulk density, thermal inertia, albedo, or spin rate markedly different from assumptions.

Finally, there are a number of asteroids showing a significant signal for nongravitational acceleration, and yet with a magnitude too great to be attributed to the Yarkovsky effect. We term these "spurious detections" because most are due to erroneous optical astrometry, often involving a single isolated night from precovery observations. Some cases may be due to other nongravitational accelerations, such as outgassing, mass loss, or micro-meteoroid flux.

Keywords. Asteroids, ephemerides

1. Introduction

The Yarkovsky effect is a slight nongravitational acceleration on asteroids due to anisotropic thermal emissions. The effect derives from the fact that thermal inertia causes an asteroid's evening terminator to be warmer than the morning terminator, leading to a net excess of thermal photons emitted from the evening terminator and a resultant net recoil acceleration towards the morning terminator. For asteroids in direct rotation the Yarkovsky effect produces a mean acceleration along the velocity vector, leading

to a steady increase in orbital energy and an outward drift in orbital semimajor axis. Retrograde rotators have a deceleration with respect to the orbital velocity and so the semimajor axis drift is inwards.

The acceleration due to the Yarkovsky effect is exceedingly minute and yet can have significant effects on an asteroid's orbit. As an example, consider 101955 Bennu, a typical half-kilometer Near-Earth Asteroid (NEA). The magnitude of the transverse acceleration (the component that matters) on Bennu is of order 10^{-12} m/s^2, which leads to a semimajor axis drift of only 284 m/yr, and yet causes hundreds of kilometers of along-track orbital drift in less than 20 years (Chesley *et al.* 2014). This is because a linear drift in semimajor axis (and orbital period) produces a quadratic-in-time drift in the orbital anomaly, which is the clearest manifestation of the Yarkovsky effect.

In the modern literature the Yarkovsky effect was first described by Öpik (1951), who attributed it to a lost pamphlet written Ivan Yarkovsky, a Polish civil engineer working in Russia. Later Beekman (2006) re-discovered the lost manuscript. In recent decades the Yarkovsky effect has become a central element of our current understanding of asteroid dynamical evolution. It is key to explaining a host of phenomona, from the cosmic ray exposure ages of meteorites (Farinella *et al.* 1998), to the delivery of NEAs from the main belt to the inner solar system (Farinella & Vokrouhlický 1999; Morbidelli & Vokrouhlický 2003), to to the structure of asteroid families (Bottke *et al.* 2001), just to name a few. See Bottke *et al.* (2006) for a complete discussion of the theory, history and implications of the Yarkovsky effect.

The first direct detection of the Yarkovsky effect on a specific asteroid was for 6489 Golevka (Chesley *et al.* 2003), and since that time the number of detections has steadily increased. The earliest scans of the NEA catalog found 10 detections in 2008 (Chesley *et al.* 2008), and later work increased the number of detections to 13 (Nugent *et al.* 2012), and then 21 (Farnocchia *et al.* 2013) and 37 detections as of December 2014 (Vokrouhlický *et al.* 2015). Less than one year later we now report 42 detections as detailed below. This steady growth in the number of detections is due to the naturally increasing arc length of discovered NEAs as time passes, as well as to expanded efforts in radar astrometry and more capable ground-based NEA search programs.

2. Technical Approach

We performed a systematic scan of the NEA catalog for signs of the Yarkovsky effect in the orbital motion of individual objects. We used published optical[1] and radar[2] astrometry as of 17 July 2015 to estimate the transverse nongravitational acceleration for the 5095 NEAs with data arcs longer than 100 days.

Our Yarkovsky effect model assumes a $1/r^2$ thermal emission model, where r is the asteroid's heliocentric distance. The associated model for transverse acceleration is

$$a_T = A_2 \left(\frac{r_0}{r}\right)^2,$$

where $r_0 = 1$ au is a normalizing constant and A_2 is an estimable parameter. For each object considered we estimate A_2 concurrently with the osculating orbital elements at epoch. The A_2 estimate leads directly to an estimate of the mean semimajor axis drift

[1] Optical astrometry was derived from the Minor Planet Center (MPC) online data, which can be obtained from `http://minorplanetcenter.net`.

[2] Radar astrometry was obtained from the JPL radar database available at `http://ssd.jpl.nasa.gov/?radar`

https://doi.org/10.1017/S1743921315008790 Published online by Cambridge University Press

rate

$$\langle da/dt\rangle = \frac{2A_2(1-e^2)}{n}\left(\frac{r_0}{p}\right)^2,$$

where e denotes the orbital eccentricity, n the mean motion and p the semilatus rectum (Farnocchia *et al.* 2013). The uncertainty $\sigma_{\langle da/dt\rangle}$ is obtained analogously from the A_2 uncertainty σ_{A_2}.

To discern the significance of any estimated semimajor axis drift rate we consider the signal-to-noise ratio

$$\mathrm{SNR} = \left|\frac{\langle da/dt\rangle}{\sigma_{\langle da/dt\rangle}}\right|.$$

We must also understand whether the estimated $\langle da/dt\rangle$ is physically realistic and consistent with the presumed Yarkovsky mechanism. Thus we also compute $\mathrm{SNR}_{\max}$, which denotes the maximum SNR that may be obtained from the Yarkovsky effect by assuming extremal obliquity and other parameters favorable to a maximal $|\langle da/dt\rangle|$. Finally, we define the parameter $\mathcal{S} = \mathrm{SNR}/\mathrm{SNR}_{\max}$, which is a rough proxy for cosine of obliquity, assuming that the diameter, density and thermal properties are not markedly different from the assumptions. The interpretation of $\mathcal{S}$ is that value of 1 indicates an estimated Yarkovsky drift that is roughly at the maximal level. A value significantly greater than 1 indicates a semimajor axis drift rate that is incompatible with the Yarkovsky effect, and a value significantly less than 1 points to a weak drift.

3. Results

The results of our comprehensive search for detectable Yarkovsky effect among the NEAs are depicted in Fig. 1, where SNR vs. $\mathrm{SNR}_{\max}$ is plotted for each object considered. For select cases the object designation is also depicted adjacent to the respective point on the plot. In this space we can readily divide the population into four categories as follows:

No signal. For the vast majority (97%) of NEAs considered we have both $\mathrm{SNR} < 3$ and $\mathrm{SNR}_{\max} < 3$, indicating that no Yarkovsky signal is expected and none is found. This is not surprising given that we have included a large number of objects in the scan to ensure that no interesting cases were missed. Indeed, most objects considered have a limited observational data set that is unlikely to reveal any nongravitational acceleration.

Valid detections. NEAs with $\mathrm{SNR} \geqslant 3$ are considered detections, but only those with $\mathcal{S} < 1.5$ are considered valid. We have 42 valid detections for the NEA catalog as of July 2015. These are detailed in Table 1 and discussed below.

Spurious detections. The "spurious" Yarkovsky detections are those with $\mathrm{SNR} \geqslant 3$, but with $\mathcal{S} \geqslant 1.5$, which indicates that $|\langle da/dt\rangle|$ is at least 50% greater than one would reasonably expect for the Yarkovsky effect. We have 60 such cases, all but two of which have $\mathrm{SNR} < 7$.

Weak detections. These "detections" of a weak Yarkovsky drift are those for which $\mathrm{SNR} < 3$, but $\mathrm{SNR}_{\max} > 3$ (and $1/\mathcal{S} > 1.5$). This indicates that if the Yarkovsky effect were maximized for an object of this size the semimajor axis drift would be detectable, and yet these objects do not show a detectable drift. As we discuss below, there are a number of reasons for a weak Yarkovsky effect, e.g., obliquity near 90°, which tends to null the Yarkovsky effect. Table 2 lists the objects with a weak Yarkovsky effect. Of the 42 objects in this category we only tabulate the eight cases with $\mathcal{S} < 0.1$, i.e., those for which the Yarkovsky effect is $< 10\%$ of its presumed maximal value.

https://doi.org/10.1017/S1743921315008790 Published online by Cambridge University Press

Table 1. List of Valid Yarkovsky Detections as of July 2015.

Object		$\bar{r}$ (au)	H	D (m)	$\langle da/dt \rangle$ (10^{-4} au/My)	SNR	$\mathcal{S}$	Data Arc	$N_{\rm rad}$
101955	Bennu	1.10	20.6	493	−18.954 ± 0.097	194.6	1.00	1999-2013	3
2340	Hathor	0.75	20.2	210	−17.40 ± 0.70	24.9	0.28	1976-2014	1
152563	1992 BF	0.87	19.6	510	−11.82 ± 0.56	21.0	0.56	1953-2011	0
	2009 BD	1.01	28.2	4	−484 ± 33	14.5	0.20	2009-2011	0
	2005 ES70	0.70	23.7	61	−73.2 ± 5.1	14.3	0.35	2005-2015	0
437844	1999 MN	0.50	21.4	179	43.2 ± 3.9	11.2	0.37	1999-2015	0
2062	Aten	0.95	17.1	1300	−5.54 ± 0.73	7.6	0.72	1955-2015	5
6489	Golevka	2.01	19.1	280	−4.52 ± 0.60	7.5	0.13	1991-2011	3
1862	Apollo	1.22	16.1	1400	−1.59 ± 0.24	6.6	0.19	1930-2015	2
162004	1991 VE	0.67	18.2	769	19.6 ± 3.0	6.5	0.83	1954-2015	1
377097	2002 WQ4	1.63	19.5	424	−10.1 ± 1.6	6.4	0.44	1950-2014	0
	2006 CT	1.07	22.3	119	−47.3 ± 7.6	6.2	0.59	1991-2014	1
	2000 PN8	1.22	22.1	130	49.3 ± 8.7	5.7	0.72	2000-2014	0
10302	1989 ML	1.26	19.4	248	38.7 ± 7.5	5.1	1.12	1989-2012	0
363505	2003 UC20	0.74	18.3	751	−4.36 ± 0.85	5.1	0.27	1954-2015	1
85990	**1999 JV6**	0.96	20.1	451	−19.3 ± 3.8	5.0	0.83	1999-2015	1
216523	**2001 HY7**	0.83	20.4	287	40.0 ± 8.2	4.9	0.96	2001-2015	0
3908	Nyx	1.71	17.3	1000	8.6 ± 1.8	4.7	0.99	1980-2014	2
29075	1950 DA	1.46	17.1	2000	−2.70 ± 0.57	4.7	0.55	1950-2014	2
2100	Ra-Shalom	0.75	16.1	2240	−5.7 ± 1.2	4.7	0.99	1975-2013	4
399308	1993 GD	1.07	20.7	180	43.7 ± 9.6	4.5	0.82	1993-2015	0
85953	1999 FK21	0.53	18.0	590	−11.0 ± 2.4	4.5	0.30	1971-2014	0
4034	Vishnu	0.95	18.3	420	−33.7 ± 7.5	4.5	1.23	1986-2015	1
	1995 CR	0.45	21.7	100	−331 ± 76	4.4	0.82	1995-2014	0
388189	**2006 DS14**	0.81	20.4	315	−40 ± 10	4.1	1.10	2002-2014	0
85774	1998 UT18	1.33	19.1	900	−2.63 ± 0.66	4.0	0.26	1989-2014	3
	2004 KH17	0.62	21.9	197	−40 ± 10	4.0	0.53	2004-2013	1
3361	Orpheus	1.14	19.0	348	6.4 ± 1.6	3.9	0.23	1982-2014	0
1566	**Icarus**	0.61	16.3	1300	−3.64 ± 0.95	3.8	0.16	1949-2015	3
	1994 XL1	0.57	20.8	231	−37.6 ± 9.8	3.8	0.54	1994-2011	0
425755	**2011 CP4**	0.45	21.1	200	114 ± 32	3.6	0.56	2002-2015	1
138852	2000 WN10	0.96	20.1	326	17.0 ± 4.8	3.5	0.53	2000-2014	0
4581	Asclepius	0.96	20.8	240	−20.0 ± 5.7	3.5	0.45	1989-2015	1
	1999 SK10	1.58	19.6	400	−23.5 ± 6.7	3.5	1.06	1999-2014	0
66400	1999 LT7	0.70	19.4	411	−33.6 ± 9.7	3.4	0.90	1987-2014	0
	2007 TF68	1.36	22.7	99	−60 ± 18	3.4	0.69	2002-2012	0
	1999 FA	1.07	20.6	300	−43 ± 13	3.3	1.37	1978-2008	0
256004	2006 UP	1.51	23.0	85	−71 ± 22	3.3	0.73	2002-2014	0
350462	1998 KG3	1.15	22.2	125	−25.4 ± 7.8	3.2	0.35	1998-2013	0
138175	**2000 EE104**	0.96	20.2	310	−28.9 ± 9.1	3.2	0.86	2000-2015	1
4179	Toutatis	1.96	15.1	2800	−1.81 ± 0.60	3.0	0.51	1934-2015	5
54509	**YORP**	0.97	22.6	100	−41 ± 13	3.0	0.41	2000-2005	2

NOTE. — Reliable detections with SNR larger than 3 are listed. $\bar{r} = a\sqrt{1-e^2}$ is the solar flux-weighted mean heliocentric distance. The diameter D is derived from the literature when available or from absolute magnitude H with 15.4% albedo. The da/dt and 1-σ formal uncertainty are derived from the orbital fit. $N_{\rm rad}$ denotes the number of radar apparitions in the fit. Objects listed in **bold** are recent additions since Vokrouhlický *et al.* (2015).

https://doi.org/10.1017/S1743921315008790 Published online by Cambridge University Press

Table 2. List of Weak Yarkovsky Detections as of July 2015.

Object		$\bar{r}$ (au)	H	D (m)	$1/\mathcal{S}$	Data Arc	$N_{\rm rad}$
247517	2002 QY6	0.58	19.6	269	441.29	2002-2014	0
161989	Cacus	1.10	17.1	1126	56.68	1978-2015	0
152742	1998 XE12	0.59	19.0	413	27.22	1995-2014	0
277810	2006 FV35	0.93	21.6	160	26.22	1995-2015	0
	2000 TH1	1.94	22.4	110	25.16	2000-2014	0
225312	1996 XB27	1.19	21.7	84	19.71	1996-2014	0
3757	Anagolay	1.64	19.1	390	16.98	1982-2014	1
5797	Bivoj	1.70	18.8	500	13.04	1953-2014	0

NOTE — Weak detections with $1/\mathcal{S} > 10$ are listed. Column descriptions are as in Table 1.

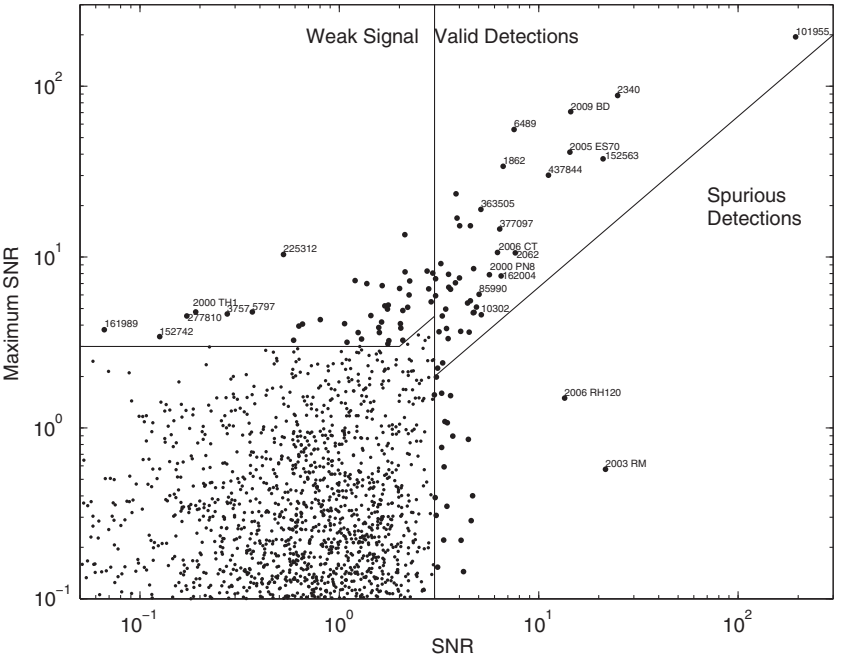

Figure 1. Yarkovsky effect detections are revealed in a plot of maximum (based on size only) vs. detected SNR. Weak cases show no evidence of Yarkovsky semimajor axis drift although a detectable drift is in principle possible. Both valid and spurious detections show SNR > 3, but the spurious cases have SNR $> 1.5 \times \mathrm{SNR}_{max}$.

4. Discussion

4.1. *Valid Detections*

Among our 42 valid detections of the Yarkovsky effect (Table 1) there are 32 with $\langle da/dt \rangle < 0$, which suggests roughly 75% retrograde rotators among our sample. This is in accord with previous results (e.g., Farnocchia *et al.* 2013), and is believed to be an indication that the ν_6 resonance in the main asteroid belt is the primary source of small NEAs (La Spina *et al.* 2004). The ν_6 resonance is near the inner edge of the main belt, and so main belt asteroids must be drifting inwards to enter that resonance, thus all ν_6

https://doi.org/10.1017/S1743921315008790 Published online by Cambridge University Press

objects are retrograde. For other source regions, asteroids can drift outwards or inwards to the resonances and so objects arriving through these resonances are expected to have parity between retrograde and direct rotation. With this idea and our current results, we infer that roughly half of our sample was delivered through the ν_6 resonance. See Farnocchia *et al.* (2013) for a more statistically rigorous analysis.

We can compare the current list of detections with that reported from December 2014 by Vokrouhlický *et al.* (2015). The new list has lost two cases with lower significance, namely 2063 Bacchus, which fell from SNR = 3.2 to 1.3 with the incorporation of radar astrometry from 2015, and 37655 Illapa, which fell from SNR 3.0 to 2.9 with the addition of 2015 optical astrometry. On the other hand, we have gained seven new objects, which we mark with bold font in Table 1. Two of the new cases (1566 Icarus and 85990 1999 JV6) have new radar astrometry in 2015 and another three have an additional optical apparition in 2015. Many of the results have changed slightly since the last run because we have implemented a different weighting and debiasing scheme for the optical astrometry as described by Farnocchia *et al.* (2015), which leads to small shifts in the estimates.

Additional remarks:

• Of special note is the case of 4179 Toutatis, which dropped from SNR 8.4 to 3.0 as a result of a number of revisions in the list of the radar range measurements reported for this object (J. Giorgini, private communication).

• 433 Eros initially appears as valid, with SNR = 3.1 and $\mathcal{S} = 1.4$, however, the obliquity of Eros is $\gamma \simeq 90^\circ$, which means that the detection is certainly spurious, and we have moved it to that category. The Eros orbit estimate is extraordinarily precise as a result of a data arc extending back to 1893, and we suspect that subtle modeling issues such as reference frame stability are responsible for the spurious detection.

• The strongest detection remains that of 101955 Bennu. This is also the first case where a bulk density has been derived from a Yarkovsky detection (Chesley *et al.* 2014).

• For all of the valid detections for which the obliquity of the asteroid has been derived through observations, we find agreement between the sign of $\langle da/dt \rangle$ and the sign of $\cos\gamma$, reinforcing our conclusion that the Yarkovsky effect is the cause of the detected orbital deviations.

• More than half of the valid detections could also be considered weak detections because $1/\mathcal{S} > 1.5$, which is not unreasonable in light of the discussion on weak detections below.

4.2. *Spurious Detections*

Detections with $\mathcal{S} > 1.5$ are presumably spurious for some reason, generally erroneous astrometry. We have 60 cases in this category, including 433 Eros, as mentioned above. With a naive or automated statistical treatment of the astrometry there can be many more spurious detections, but we have manually treated numerous cases where a precovery, i.e., a short apparition (typically only 1–2 nights) that is isolated in time from the bulk of the observations, has an inordinate effect on the Yarkovsky estimate. These are cases where astrometric errors (often in the form of clock errors at the telescope) can easily lead to a spurious Yarkovsky detection and the astrometry is not independently confirmed by other observers in nearby nights. In such cases, de-weighting the observations in question increases $\sigma_{\langle da/dt \rangle}$ and the SNR falls accordingly.

However, in at least two cases neither the Yarkovsky effect nor astrometric errors can explain the large and significant da/dt values and we suppose some other nongravitational acceleration is at play, e.g., outgassing or mass shedding. We describe these two cases below.

https://doi.org/10.1017/S1743921315008790 Published online by Cambridge University Press

2003 RM: This object, nominally 380 m in diameter, shows SNR $\simeq 22$ and $\mathcal{S} \simeq 38$, and thus we have an acceleration with very high statistical confidence that is 38× greater than the Yarkovsky effect could produce. However, the orbit of 2003 RM is similar to many comet orbits, with aphelion distance of 4.7 au and a Jupiter Tisserand parameter of 2.96, suggesting that cometary outgassing could be responsible for the large and significant nongravitational accelerations. There are a number of NEA survey programs (specifically, MPC observatory codes F51, E12, 703, 691) who reported observations of 2003 RM near past perihelia. Each of these programs report that, while 2003 RM seems to appear slightly more diffuse than nearby stars, there is no unambiguous evidence for a coma in the original images (E. Christensen, R. McMillan, R. Wainscoat; private communication). We believe that this object is cometary and predict that detailed observations taken with a 2-meter class telescope at the next perihelion in mid-2018, when it is well-situated for ground-based observations, will reveal cometary activity.

2006 RH120: This is a tiny asteroid, roughly 3 m in diameter (at 28% albedo), that was temporarily captured by the Earth-Moon system and remained bound for several months. Because of its small size and unusual orbit there was some early speculation that this object could be an artificial object left over from a space mission. However, the 2006 RH120 orbit reveals a radial acceleration, presumably due to direct solar radiation pressure, that indicates an area-to-mass ratio of $(5.5 \pm 0.2) \times 10^{-4}$ m^2/kg, a value clearly inconsistent with an artificial object. For a 3 m diameter sphere this area-to-mass ratio would imply a bulk density of roughly 900 kg/m^3, which is low, but not implausibly so for a natural object. The detected transverse acceleration has SNR $\simeq 13$ and $\mathcal{S} \simeq 9$, indicating a real acceleration that is $\sim 9\times$ more than the Yarkovsky effect allows. We do not have a good hypothesis to explain the high transverse acceleration, but we suppose it should be explained by one of the following issues:

- A lack of fidelity in the gravitational force model,[3]
- A lack of fidelity in the thermal modeling for such small objects,
- Unrecognized astrometric error,
- Some other nonconservative force, e.g., mass-shedding or outgassing. Or micrometeorite flux, for which Wiegert (2015) suggests that the ejecta recoil acceleration could be almost as great as the Yarkovsky effect for objects on similar orbits in this size range.

The first three of these do not appear as reasonable explanations to us, and so we speculate that the last item is the most likely.

4.3. *Weak Detections*

Cases with $\mathrm{SNR}_{\max} > 3$ and $\mathrm{SNR} < 3$ are indicative of a Yarkovsky effect that is markedly weaker than the maximum obtained for the assumed asteroid size. We note that

$$\langle da/dt \rangle \propto \frac{\cos\gamma}{\rho D},$$

where γ is the obliquity of the asteroid equator. Thus, $\mathcal{S} \simeq |\cos\gamma|$ if the diameter D and bulk density ρ are not significantly different from the assumed values. Moreover, inconsistencies in additional parameters associated with the thermal model (such as thermal inertia, rotation rate and Bond albedo) could also cause modest deviations in

[3] Our dynamical model assumes point masses for the eight planets plus the Moon, Pluto and the 16 largest main belt asteroids. We also include the Earth's J_2, which should be adequate for an object that did not approach the Earth closer that 0.7× the lunar distance during its observed arc. We include general relativity perturbations for the sun, the eight planets and the Moon.

https://doi.org/10.1017/S1743921315008790 Published online by Cambridge University Press

$\mathcal{S}$. Such inconsistencies do dilute the interpretation of $\mathcal{S}$ as a proxy for $|\cos\gamma|$ and yet if $\mathcal{S}$ is small enough, say less than 0.1, then it is generally safe to infer $|\cos\gamma| \ll 1$. Such cases are presumably indicative of midrange obliquity, which tends to null the Yarkovsky effect, a hypothesis that we are testing through an observational program to estimate spin axis orientations for some of the objects in this category.

5. Summary

We have identified 42 NEAs with valid Yarkovsky detections, including seven new cases within the past year, suggesting that the list of valid detections will continue to grow at a rapid pace. The average since 2003 is 3.5 new valid detections per year. We note that over 75% of the valid detections show $\langle da/dt\rangle < 0$ indicating retrograde rotation, which continues to reinforce the prevailing understanding that the ν_6 resonance is the dominant source region for NEAs.

We have 60 spurious detections, most of which presumably stem from astrometric errors. We find that 72% of spurious cases have SNR < 4 and only 8% have SNR > 5. Among the latter group we have two cases with SNR > 10 that cannot be explained by the Yarkovsky effect nor by erroneous astrometry. The implication for these is that there must be some other un-modeled acceleration acting on the body that exceeds that of the Yarkovsky effect.

Finally, we have 42 weak detections, which are actually non-detections with $\mathrm{SNR}_{\max} > 3$. These are the cases that the Yarkovsky effect is markedly less than it could be for the assumed asteroid size. Of these there are 8 cases with $1/S > 10$, including one case with $1/S \sim 440$.

Acknowledgements

This research was conducted in part at the Jet Propulsion Laboratory, California Institute of Technology, under a contract with the National Aeronautics and Space Administration. The work by P.P. and D.V. was supported by the Grant Agency of the Czech Republic, Grant P209/12/0229.

References

Beekman, G. 2006, *Journal for the History of Astronomy* 37, 71

Bottke, W. F., Vokrouhlický, D., Broz, M., Nesvorný, D., & Morbidelli, A. 2001, *Science* 294, 1693

Bottke, W. F., Jr., Vokrouhlický, D., Rubincam, D. P., & Nesvorný, D. 2006, *Annual Review of Earth and Planetary Sciences* 34, 157

Chesley, S. R., Farnocchia, D., Nolan, M. C., Vokrouhlický, D., Chodas, P. W., Milani, A., Spoto, F., Rozitis, B., Benner, L. A. M., Bottke, W. F., Busch, M. W., Emery, J. P., Howell, E. S., Lauretta, D. S., Margot, J.-L., & Taylor, P. A. 2014, *Icarus* 235, 5

Chesley, S. R., Ostro, S. J., Vokrouhlický, D., Čapek, D., Giorgini, J. D., Nolan, M. C., Margot, J.-L., Hine, A. A., Benner, L. A. M., & Chamberlin, A. B. 2003, *Science* 302, 1739

Chesley, S. R., Vokrouhlický, D., Ostro, S. J., Benner, L. A. M., Margot, J.-L., Matson, R. L., Nolan, M. C., & Shepard, M. K. 2008, *LPI Contributions* 1405, 8330

Farinella, P. & Vokrouhlický, D. 1999, *Science* 283, 1507

Farinella, P., Vokrouhlický, D., & Hartmann, W. K. 1998, *Icarus* 132, 378

Farnocchia, D., Chesley, S. R., Chamberlin, A. B., & Tholen, D. J. 2015, *Icarus* 245, 94

Farnocchia, D., Chesley, S. R., Vokrouhlický, D., Milani, A., Spoto, F., & Bottke, W. F. 2013, *Icarus* 224, 1

La Spina, A., Paolicchi, P., Kryszczyńska, A., & Pravec, P. 2004, *Nature* 428, 400

Morbidelli, A. & Vokrouhlický, D. 2003, *Icarus* 163, 120
Nugent, C. R., Margot, J. L., Chesley, S. R., & Vokrouhlický, D. 2012, *AJ* 144, 60
Öpik, E. J. 1951, *Proc. R. Irish Acad. Sect. A* 54, 165
Vokrouhlický, D., Bottke, W. F., Chesley, S. R., Scheeres, D. J., & Statler, T. S. 2015, in: P. Michel, F. DeMeo & W. F. Bottke (eds.), *Asteroids IV*, Univ. Arizona Press, Tucson, 509–531
Wiegert, P. A. 2015, *Icarus* 252, 22